

Biomolecular Effects of Cold Plasma Exposure

Rakesh Mogul*, Alexander A. Bol'shakov^{†‡}, Suzanne L. Chan*, Ramsey D. Stevens[§],

Bishun N. Khare[¶], M. Meyyappan^{||}, Jonathan D. Trent***

*Astrobiology Technology Branch, NASA ARC Moffett Field, CA 94035; [†]Plasma
Research Group, NASA ARC, Moffett Field, CA 94035; [§]Eloret Co., Sunnyvale, CA
94087; [¶]SETI Institute, Mountain View, CA. 94043; ^{||}Center for Nanotechnology, NASA
ARC, Moffett Field, CA 94035

The effects of cold plasma exposure on *Deinococcus radiodurans*, plasmid DNA and model proteins were assessed using microbiological, spectrometric and biochemical techniques. Exposure of *D. radiodurans*, an extremely radiation resistant microbe, to O₂ plasma (≤ 25 W, ~ 45 mTorr, 90 min) yielded a ~ 99.999 % sterilization and the sterilization rate was increased ~ 10 -fold at 100 W and 500 mTorr. AFM images shows that the exposed cells are significantly deformed and possess 50-70 nm concavities. IR analysis indicates the chemical degradation of lipids, proteins and carotenoids of the cell wall and membrane. Intracellular damage was indicated by major absorbance loss at 1245, 1651 and 1538 cm⁻¹ corresponding to degradation of DNA and proteins, respectively. Biochemical experiments demonstrate that plasmas induce strand scissions and crosslinking of plasmid DNA, and reduction of enzyme activity; the degradation is power dependent with total sample loss occurring in 60 s at 200 W and 500 mTorr. Emission spectroscopy shows that *D. radiodurans* is volatilized into CO₂, CO, N₂ and H₂O confirming the removal of biological matter from contaminated surfaces. The O₂ plasma impacts several cellular components predominantly through chemical degradation by atomic oxygen. A CO₂ plasma, however, was not effective at degrading *D.*

radiodurans, revealing the importance of plasma composition, which has implications for

lower
page

Planetary Protection and the contamination of Mars.

Introduction

The sterilization and removal of biological matter from contaminated surfaces is of significant interest to medicine (1, 2) and the NASA Planetary Protection guidelines (3, 4). The inactivation of microorganisms and biological molecules can be accomplished through a variety of established techniques including thermal, chemical and/or radiation treatments (5-7). Recent improvements in detection methods for microorganisms and biomolecules, however, have revealed unforeseen resistances to these established treatments (8-11) and have thus prompted the development of new techniques and procedures (12-16). Among these new techniques is the use of low temperature plasmas, which have gained substantial recognition in the medical industry due to their efficacy and low costs (17-20). Plasmas generated from gasses such as O₂, N₂, CF₄, CO₂ and air are generally characterized by non-thermal kinetic equilibrium processes that result in the production of neutral and ionic species, free electrons and UV radiation. These plasmas typically induce low surface temperatures (< 100 °C) and effectively sterilize common microbes such as *S. aureus*, *E. coli*, *B. subtilis* and *B. stearothermophilus*. Cold plasmas therefore are ideal for the surface sterilization and cleaning of devices that are sensitive to other established procedures.

Effective sterilization protocols are of interest to NASA due to the potential contamination of planets such as Mars and Europa due to exploration using space probes designed to study chemical evolution and the origin of life (3, 21). This type of forward contamination would result in the interference of life-detecting probes as well as impact to extraterrestrial ecosystems (22, 23). Of particular concern, are the microorganisms, viruses and biomolecules that can survive in the low-pressure and high-radiation

environments of interplanetary space and potentially on the surfaces of Mars or Europa. An ideal biological example is the highly desiccation resistant microbe, *Deinococcus radiodurans*, which can survive in radiation environments of 60 Gy/h for 30 h with no loss in viability (24-26).

We have studied *D. radiodurans* and other model biomolecules with the specific aims to address the efficacy of O₂ plasmas against a radiation resistant microorganism and to gain insights into the molecular effects of the exposure. The degradation of organic matter by plasma processes is known to proceed through several mechanisms including chemical degradation, sputtering and UV photodesorption (27). While the respective biological effects of many reactive oxygen species (28-30) and UV radiation (31, 32) have been studied in great detail, the molecular interactions between low-temperature plasmas and biological matter have yet to be elucidated. Our experimental strategy therefore has provided a more thorough understanding of how plasma power and processes contribute to the sterilization, degradation and removal of biological matter.

Materials and Methods

Materials. *D. radiodurans* R1 was obtained from ATCC and stored as glycerol stocks at -80°C. Growth media were prepared as described (25). Plasmid DNA (pRc/CMV2) and BSA were purchased from Sigma. Soybean lipoxygenase-1 (SLO) and linoleic acid (LA) were obtained from the Holman Research Group (U.C. Santa Cruz). Oxygen gas was purchased from AirGas (99.9 %) and Scott Specialty Gases (99.99 %). A Martian atmospheric gas analog (MAG) containing 95.48% CO₂, 2.51% N₂ and 2.01% Ar was obtained from Matheson Gas. Hanging drop slides were obtained from Fisher Scientific.

Potassium bromide (KBr) optical windows (25 mm x 4 mm) were purchased from Harrick Scientific Corporation. All other reagents and materials were of highest grade; pure water ($18\text{ M}\Omega\text{ cm}^{-1}$) was used throughout.

Plasma Reactors. Two different plasma reactors were employed in this study: a low power ($\leq 25\text{ W}$) barrel reactor (PLASMOD, Tegal Corporation) was used for a majority of the microbiological experiments and a custom-built reactor (ARC-PR), with optimal running conditions of $\geq 50\text{ W}$, was used for experiments involving molecular and structural characterizations. In all cases, the plasmas were capacitively coupled, powered by a 13.56 MHz radio frequency (RF) and low temperature (T_e 5-12 eV). The ARC-PR was constructed by the plasma research group at the NASA Ames Center for Nanotechnology and was designed to allow high-throughput exposures of biological samples due to the use of two connecting chambers, a load-lock and reaction chamber, which were separated by a moveable gate. Typically, the biological sample was placed into the load-lock chamber, the pressure reduced to $\sim 20\text{ mTorr}$ and the target gas introduced to final pressure of 500 mTorr. The gate was then opened and the sample moved into the reaction chamber, which contained the stabilized plasma discharge. After exposure, the sample was shifted back to the load-lock chamber, the gate closed and the pressure readjusted to 1 atm using dry air. Samples were then analyzed using microbiological, spectrometric and/or biochemical techniques. A thermocouple on the lower electrode was used to measure the surface temperatures during the plasma exposures. In all cases, the plasmas were tuned to yield a reflected power of $< 3\%$ of the forward incident power. Power is reported as the difference between the incident and reflected powers.

Microbe Exposure. *D. radiodurans* was grown in TGY media to mid-log phase ($\sim 10^8$ cells/ml) at 30 °C. Cells were diluted to 5×10^7 cells/ml in minimal media and 100 μ l were transferred onto a 25 mm (0.4 μ m) Nuclepore membrane and dried by placement onto a 7.0 cm Whatman filter. The inoculated membrane was then transferred to a glass petri dish and inserted into the PLASMOD reactor. The pressure within the reactor was reduced to ~ 20 mTorr and O₂ introduced at a flow rate of 1.02 cc/min to a final pressure of ~ 45 mTorr. The chamber was equilibrated for ~ 30 min, the RF power was applied (≤ 25 W) and the inoculated membrane exposed to the plasma for differing times (10-90 min). After exposure, the membrane was placed into 0.5 ml minimal media, gently vortexed to remove the cells and serial dilutions plated onto TGY/agar plates. Plates were incubated for 3 days at 30 °C, colonies were counted and survival assayed using the most probable numbers method. Control experiments assaying the effects of drying, reduced pressure and O₂ flow on the survival of the cells were also run. An additional survival experiment was performed using the ARC-PR at 100 W and 500 mTorr for 60 s. All experiments were done in triplicate.

Atomic Force Microscopy. A fresh mid-log phase culture of *D. radiodurans* was harvested by centrifugation (10,000 rpm, 30 s), resuspended in water and the procedure repeated twice. A suspension of $\sim 7 \times 10^9$ cells/ml was prepared in water and 10 μ l transferred onto two different coupons of freshly cleaved mica (~ 1 cm²). The coupons were dried through absorption of the excess liquid using a lint-free wiper followed by exposure to a moderate vacuum. The dried coupons were transferred to the ARC-PR and exposed to a 100 W, 500 mTorr O₂ plasma or 500 mTorr of O₂ gas (no power) for 3 min

each. Samples were then imaged using a Digital Instruments multimode atomic force microscope in tapping mode using a multi-walled carbon nanotube tip (33).

Infrared Spectroscopy. A ~ 40 ml mid-log phase culture of *D. radiodurans* was harvested (7000 rpm, 5 min) and the cell pellet completely resuspended in 30 ml 150 mM NaCl. Washing procedure was repeated twice to remove all constituents of the growth media and the final cell pellet stored at – 80 °C. Suspensions of ~ 10^{11} cell/ml were prepared by resuspending ~10-40 mg of the cells in ~ 20-70 μ l 150 mM NaCl. Microbial films were prepared onto hanging drop slides by addition of 6-8 μ l of the suspension followed by drying under moderate vacuum. The dried samples (~ 10^9 total cells) were exposed to O₂ or MAG plasmas using the ARC-PR at 100 W and 500 mTorr for 45 min. Control experiments using 500 mTorr of either gas with no applied power were also performed. Upon completion, the dried films were resuspended in 20-30 μ l water and transferred to 1.5 ml tubes. The suspensions were reduced to ~ 5 μ l using an Eppendorf vacufuge and 10 μ l MeOH were added to each sample. The methanolic suspensions were then transferred to KBr optical windows and immediately dried under vacuum to a final pressure of ~ 17 mTorr before spectroscopic analysis. The infrared absorption of each sample was measured between 400–4000 cm⁻¹ using a Nicolet Nexus FT-IR 670 *e.s.p.* spectrophotometer (2 cm⁻¹ resolution, 64 scans). All reactions were done in triplicate.

Emission Spectroscopy. A SpectraPro 300i spectrometer (Acton Research) with a SpectruMM CCD Detector (Roper Scientific) was fixed ~ 35 cm in front of the reaction chamber of the ARC-PR. The light emitted from the plasma was focused using a quartz lens and the emission spectrum recorded between 280–930 nm in three steps: (1) 280-400 nm with no filter, (2) 400-700 nm using a 375 nm cutoff filter and (3) 700-930 nm using

a 650 nm cutoff filter. These glass filters were introduced directly in front of the spectrograph slit to eliminate the second order diffraction of the grating (1200 g/mm). Inverse linear dispersion of the instrument was 2.7 nm/mm, entrance aperture ratio was 0.25 f and slit widths were normally 0.2 mm. Emission spectra for both the O₂ and MAG plasmas at 100 W and 500 mTorr were recorded.

Fresh mid-log phase cultures (2 ml) of *D. radiodurans* were harvested (14,000 rpm, 30 s) and thoroughly resuspended in 1 ml water. Washing procedure was repeated three times to remove all constituents of the growth media and the final cell pellet was resuspended in 30 μ l water. The suspension was transferred to hanging drop slides (~ 10⁹ total cells) and dried under moderate vacuum. A control sample was also prepared using 30 μ l of water (no microbes). Samples were exposed to the O₂ plasma at 100 W and 500 mTorr in a closed system. The emission spectra of the plasma discharge were recorded immediately upon exposure of the sample and repeated in 3-10 min increments over the course of ~ 40 min. At the end of the exposure, the pressure within the reaction chamber had risen to ~ 650 mTorr indicating conversion of the biological matter into the gas phase. Spectra of two duplicate microbial exposures were compared for reproducibility and against the water control to reveal any background contamination.

DNA and protein exposure. Plasmid DNA, BSA and SLO were exposed to O₂ or MAG plasmas at differing powers and the effects assayed using electrophoresis or spectroscopy. Plasmid DNA (pRc/CMV2, 5.5 kb) was dissolved in water to 0.5 μ g/ μ l and added onto hanging drop slides in 2 μ l aliquots. The DNA containing slides were dried under moderate vacuum, transferred to the ARC-PR and exposed to 50-200 W of either plasma for 60 s each. Control experiments were also performed by exposing the dried

DNA samples to 500 mTorr of the target gas (no power) and by heating the samples to 76 °C or 55 °C for 60 s each. After exposure, each sample was dissolved in 12 μ l 25 mM HEPES (pH 8.0), and 10 μ l transferred to a 1.5 ml tube containing 2 μ l of 6x DNA running dye. All samples were analyzed in parallel by electrophoresis at 80 V using a 0.8 % agarose gel in TAE with 0.25 μ g/ml ethidium bromide. Gels were visualized by fluorescence (λ_{ex} 302 nm), images were captured and the DNA bands quantified using a UVP Laboratory Imaging and Analysis System. DNA sizes were estimated by comparison to a 1 kb DNA molecular weight ladder (Invitrogen) and the percent change in each DNA band calculated by comparison to the control. All reactions were done in duplicate.

BSA was dissolved into water (1 mg/ml), dried onto hanging drop slides in 10 μ l aliquots and exposed to the O₂ plasma (50-250 W, 500 mTorr, 90 s). After exposure, samples were dissolved in 20 μ l 25 mM HEPES (pH 8.0); 10 μ l were then removed, mixed with 5 μ l 4x SAE/BME and adjusted to 20 μ l. All samples were heated at 95 °C for 5 min and separated under denaturing conditions at 150 V using 8-16 % polyacrylamide gradient gel (ISC BioExpress). Gels were stained using Coomassie Brilliant Blue and imaged as described. SLO (1 mg/ml) was added onto hanging drop slides in 5 μ l aliquots, dried under moderate vacuum and exposed to the O₂ plasma (50-200 W, 500 mTorr, 60 s). After exposure, each sample was dissolved in 22 μ l 100 mM sodium borate (pH 9.2); 20 μ l were then removed and diluted to 500 μ l. Enzymatic activities were measured using ~ 42 μ M LA in 2 ml 100 mM sodium borate (pH 9.2). Kinetic reactions were initiated by addition of 100 μ l enzyme and the change in absorbance at 234 nm monitored using an Amersham Pharmacia Ultraspec 3300 pro

UV/Vis spectrophotometer. Enzymatic rates were determined by calculation of the initial slopes using the Swift II application software. Control experiments were performed by heating samples at 76 °C for 90 or 60 s. All reactions were done in duplicate.

Results

Microbe exposure. *D. radiodurans* cultures were dried onto polycarbonate membranes and exposed to the O₂ plasma (≤ 25 W, ~ 45 mTorr) for 10, 20, 30, 60 and 90 min (Fig. 1). Control experiments indicated negligible affects as a result of drying and the reduced pressures in the plasma reactor (>95 % survival). The cell survivability in Fig. 1 is expressed in terms of percent survival as compared to the control samples. The 10 min plasma exposure yielded a ~ 0.1 % survival indicating a ~ 3 -log reduction in living cells. The survival was further reduced to ~ 0.001 % after 60 min and ~ 0.0001 % after 90 min; which translated to an overall ~ 6 -log reduction in cell survivability indicating that less than 5 cells, out of an initial 5×10^6 , remained alive after the final exposure. The observed difference in sterilization rates between the 10 and 90 min exposures was most likely due to shielding caused by the sterilized cells or the polycarbonate membrane. This shielding effect may be the reason long exposure times are necessary for complete sterilization. Using the ARC-PR at 100 W and 500 mTorr, we observed a 0.1 % sterilization after 1 min indicating that sterilization rates are effectively expedited at higher powers and pressures. Images of *D. radiodurans* were then obtained using atomic force microscopy (AFM) in order to reveal the degree of structural degradation induced by the O₂ plasma.

Atomic Force Microscopy. Insights into the mechanism of sterilization for *D.*

radiodurans were obtained by AFM in tapping mode using a multiwalled carbon nanotube tip. Images of the control (dried at low pressure) and plasma exposed cells were compared to reveal the changes in cell structure (Fig. 2A & B). In the dried, unexposed *D. radiodurans* cell cluster the individual cells are $\sim 1.75 \mu\text{m}$ in diameter, $\sim 0.5 \mu\text{m}$ in height and in direct contact with one another. In contrast, the plasma treated cell cluster (100 W, 500 mTorr, 3 min) shows each individual cell to be reduced in size, trapezoidal in shape and clearly separated from one another. Each plasma exposed cell is $\sim 1.5 \mu\text{m}$ in length, $\sim 0.5 \mu\text{m}$ in width and $\leq 0.2 \mu\text{m}$ in height. Topography maps of the unexposed and exposed cells (Fig. 2C & D) further indicated the degree of surface degradation. A high-magnification image of a single cell within each cluster (Fig. 2E & F) revealed that the surface layer (S-layer) of the unexposed cell was removed or ruptured by the plasma treatment as indicated by the major change in morphology. The $\sim 50\text{-}70 \text{ nm}$ concavities produced by the plasma exposure (Figs. 2D & F) are presumably results of the collapse of the degraded surface or by complete removal of the cell wall and membrane, thereby revealing the dried interior of the cell. The structural deformation suggested extensive chemical degradation of the microbe through the action of the O_2 plasma. The extents of this molecular damage were then assessed using infrared spectroscopy.

Infrared Spectroscopy. The infrared absorption spectra of *D. radiodurans* were measured between $400\text{-}4000 \text{ cm}^{-1}$ (Fig. 3). Dried microbial films ($\sim 3 \text{ mm}^2$) of *D. radiodurans* ($\sim 10^9$ cells) were exposed to 100 W of power at 500 mTorr of either O_2 or Mars analog gas for 45 min each. A reference spectrum of *D. radiodurans* (Fig. 3A) was obtained by performing a control experiment under identical conditions but without the

application of power. All spectra were normalized to correct for baseline and CO₂ absorption. Spectral comparison of the plasma exposed samples against the control revealed three major observations: (1) a ~ 80 % decrease in absorption for the sample exposed to the O₂ plasma (Fig. 3B), (2) a significant change in the spectral signature between 400-2000 cm⁻¹ for this sample and (3) a lack of change for the sample exposed to the MAG plasma (Fig. 3C). The ~ 80 % decrease in absorption for the O₂ plasma treated sample was attributed to the degradation and volatilization of the microbial film as a result of the O₂ plasma chemistry. The decrease in absorption at 2930 cm⁻¹ (ν, CH₂, A ~ 0.26 to 0.042) was attributed to primary reactions with the lipids and carotenoids of *D. radiodurans*. Degradation of carotenoids and other biomolecules also correlated with the visible change in the sample color and consistency from a red microbial film to a white crust-like material upon exposure. This chemical change is further supported by the difference in the IR spectrum between 400-2000 cm⁻¹. The major decrease in absorbance in the amide I/II and conjugated alkene regions (the peaks at 1651 and 1538 cm⁻¹) supported reactions with polypeptides and carotenoids. A major reduction in absorbance was also observed for the asymmetric PO₂⁻¹ stretch (1245 cm⁻¹) indicating a loss of DNA or phospholipids; as well as for the C-O stretch and out-of-plane CH bend regions (950-1200 cm⁻¹) suggesting destruction of carbohydrates and the carotenoids, respectively.

The appearance of new peaks in Fig. 3B at ~ 1650, 1384, 1121 and 981 cm⁻¹ indicated the formation of new bonds in the microbial sample. The appearance of peaks at 1384 and 1121 cm⁻¹, however, could also be potentially explained by the presence of residual methanol introduced during sample preparation. The respective peaks, however, do not match those provided in the reference spectra for methanol (1450 and 1033 cm⁻¹)

and are of opposite intensities ($I \nu, \text{OH } 3342 \text{ cm}^{-1} \cong I \nu, \text{CO } 1033 \text{ cm}^{-1} > I \delta, \text{CH}_3 \text{ } 1450 \text{ cm}^{-1}$) to those observed in the spectra in Fig. 3B ($I 1384 \text{ cm}^{-1} > I 1121 \text{ cm}^{-1} > I 3283 \text{ cm}^{-1}$) (34). In addition, neither the spectra for the control nor the MAG plasma treated sample contained these peaks, which further supported the removal of excess methanol at reduced pressures. Therefore, the new IR peaks were direct results of the chemistry between the O_2 plasma and microbial film. The change in peak ratios from 1.2 to 1.9 at 1651 and 1538 cm^{-1} can then be explained by formation of carbonyl groups on lipids and carotenoids, which would cause an increase in the relative absorbance at $\sim 1650 \text{ cm}^{-1}$. Fragmentation of these molecules could also result in an increase in the CH_3 bend, which is supported by the broad peak at 1384 cm^{-1} . The peaks at 1384 and 1121 cm^{-1} were also suggestive of oxidation of cysteine thiols into sulfonate moieties. Whereas the peaks at 1121 and 981 cm^{-1} , indicated formation of new C–O bonds within the biological sample. Taken together, these spectral differences indicated the extensive biochemical degradation and removal of *D. radiodurans* as a result of the O_2 plasma exposure. In contrast, the IR spectrum of the sample exposed to the MAG plasma (Fig. 3C) showed no detectable degradation or removal of *D. radiodurans*. This indicated a significant dependence of degradation on plasma composition. Emission spectroscopy was then performed to identify the key reactive species in the O_2 and MAG plasmas and to detect any volatile reaction products resulting from the O_2 plasma exposure.

Emission Spectroscopy. Plasma compositions were determined by recording the emission spectra between 280-930 nm before and during the microbial exposure (Fig. 4). The experimental setup involved placement of a spectrophotometer directly in front of the pyrex window of the reaction chamber of the ARC-PR. The emission spectrum for

the pure O₂ plasma discharge (Fig. 4A) indicated the presence of excited atomic oxygen, oxygen cation, dioxygen cation and neutral excited dioxygen at 100 W and 500 mTorr. Dried films of *D. radiodurans* (~ 8 mm², ~ 10⁹ cells) were then exposed to the O₂ plasma and the change in the emission spectra recorded in 3-10 min increments for a total of ~ 40 min (Fig. 4B). Comparison of the spectra indicated the formation of several excited species as a result of the degradation of *D. radiodurans*: CO₂⁺ (A²Π–X²Π system: 287-290, 312-317, 325-330, 337-344 and 351-358 nm), CO (b³Σ–a³Π and B¹Σ–A¹Π systems: 282-284, 296-298, 312-314, 329-331, 347-349, 450-452, 482-484, 518-520 and 559-562 nm), N₂ (C³Π_u–B³Π_g system: 316, 337, 357 and 380 nm), N₂⁺ (B²Σ_u–X²Σ_g system: 392 nm), OH (A²Σ–X²Π system: 306-309 nm) and H (486 and 656 nm). In addition, sodium (589 nm) and potassium (766 nm and 770 nm) emission lines were detected suggesting evidence for sputtering by the O₂ plasma. The shorter wavelengths (UV C, 100-280 nm), such as those emitted by excited phosphorous and sulfur species, were not measured due to absorption by the pyrex window. The temporal change in the emission spectra indicated that the intensities for CO₂⁺, CO and N₂ all exponentially increased with plateaus occurring ~ 20 min into exposure. Intensities for all O₂ plasma species were stable throughout the course of the experiment indicating no depletion of reactive oxygen species or parent oxygen gas. Control experiments indicated no significant inorganic and organic contamination resulting from the sample prep, glass surface or water stock. Thus, the detected carbon, nitrogen and metallic species all arose from degradation of the microbial sample.

The emission spectrum for the MAG plasma (data not shown) was also recorded and indicated that several excited species such as CO₂⁺, CO, N₂⁺, O and Ar were all

present in the plasma. Qualitatively, it was observed that the MAG plasma (as compared to the O₂ plasma) emitted lower intensities of atomic oxygen but significantly higher intensities of UV radiation due to emission from CO₂⁻ and CO. The affects of these compositional differences on the degradation and removal of biological matter were then assessed using *in vitro* biochemical experiments.

DNA and protein exposure. The extents of biochemical damage imparted by increasing powers of plasma exposure were assayed using model DNA and protein systems. Dried ~ 3 mm² films of 1 µg plasmid DNA were exposed to O₂ or MAG plasmas at 50-200 W and 500 mTorr for 60 s (Fig. 5). The increase in power for the O₂ plasma caused a concomitant rise in surface temperatures of the lower electrode in the ARC-PR from ~ 24 to 72 °C; hence, a control sample of DNA was heated to 76 °C for 60 s before analysis. Lanes 2-6 of Fig. 5A show the comparison of thermal versus O₂ plasma degradation of plasmid DNA. Upon exposure to 50 W, the amount of supercoiled DNA decreased 32 ± 1 % as compared to the thermal control, whereas the amount of nicked DNA remained constant within experimental error. Several new DNA species were produced by the plasma exposure as indicated by bands at ~ 11, 5.5, 0.5-3 kb. The ~ 11 kb band increased $\sim 14 \pm 3$ % in intensity suggesting the formation of crosslinked DNA as a result of the O₂ plasma chemistry. The appearance of a ~ 5.5 kb band indicated the formation of linear DNA as a result of either single or double stranded fragmentation of the nicked or supercoiled plasmid, respectively. Multiple double stranded fragmentation of the DNA was also indicated by the broad ~ 0.5-3 kb band. The higher power exposures of 100 and 150 W caused a ~ 5 and 20 % decrease in supercoiled DNA, respectively; indicating that ~ 50 % of the supercoiled DNA remained intact after the 150 W exposure. In contrast, the

exposure of 200 W completely degraded all DNA indicating a ~ 2-fold higher rate of degradation than that observed at 150 W. This was perhaps due to combined higher production of chemically reactive species, energetic ions, and UV radiation at 200 W.

Exposure of the dried DNA films to the MAG plasma resulted in similar degradation patterns but with differing kinetics (Fig. 5B). As a control, a sample of DNA was heated to 55 °C due to the lower surface temperatures induced under these conditions (~ 24–54 °C). Lanes 2-6 of Fig. 5B display the effects of heat and the MAG plasma on plasmid DNA. In contrast to the O₂ plasma experiments, the exposure to 50 W decreased supercoiled DNA by 48 ± 16 % and an increased nicked DNA by 8 ± 2 %. This indicated single stranded scission of the supercoiled plasmid, which increased the relative amounts of nicked DNA as compared to the O₂ plasma experiments. The 50 W exposure also caused the formation of new DNA species with sizes corresponding to ~ 11, 5.5 and 0.5-3 kb. These bands were again indicative of crosslinked, linear and multiply fragmented DNA. The most striking result of the 50 W exposure, however, was the 126 ± 6 % increase in crosslinked DNA as compared to the thermal control. The higher power exposures decreased the intensity for all DNA species yielding a 84 ± 11 % reduction in supercoiled DNA at 200 W. Therefore, the MAG plasma did not induce full degradation of the DNA but did result in more detectable fragmentations and crosslinking. Taken together, the difference in degradation rates suggested that the O₂ and MAG plasma compositions contribute differently to the degradation and removal of DNA.

The damaging effects of plasma exposure on polypeptides were also assessed using BSA and SLO (Fig. 6). The increasing powers of exposure (50-250 W) caused a non-linear decrease in the amount of BSA (Fig. 6A) and enzymatic rate of SLO (Fig. 6B)

until each parameter fell below the level of detection. The observed loss of sample and kinetic function were both attributed to oxidation, fragmentation and removal of the protein as a result of the O₂ plasma chemistry.

Discussion

The efficacy and molecular effects of low temperature O₂ plasma exposures on *D. radiodurans* and model biomolecules were assessed using microbiological, spectrometric and biochemical methods. Under very low power and pressure conditions (≤ 25 W, ~ 45 mTorr, 90 min), we have demonstrated a ~ 99.999 % sterilization of *D. radiodurans*, which is extremely resistant to both UV and gamma radiation. This effective sterilization reveals the deleterious effects of plasma species such as atomic oxygen and oxygen cation. In addition, the rates of *D. radiodurans* sterilization can be increased ~ 10 -fold at higher power and pressure (100 W, 500 mTorr) without the induction of high surface temperatures (~ 32 °C). Which indicates that plasma power can be adjusted to accommodate the sterilization of both thermolabile (low power, longer exposure times) and robust (high power, short exposure times) equipment.

The sterilization of *D. radiodurans* occurs as a combined result of damage to the cell surface, chromosome and other key intracellular components. AFM images of *D. radiodurans* show that O₂ plasma exposure completely removes or ruptures the cell wall and membrane, thereby revealing the globular interior of the cell. Infrared spectra of the exposed cells support the chemical degradation and removal of the S-layer, lipids, carbohydrates and carotenoids of the cell surface. Furthermore, the major loss in absorbance of the DNA phosphate stretch and amide I/II regions indicates that

intracellular damage to *D. radiodurans* also occurs as a result of the plasma exposure. Biochemical experiments indicate that the plasma (at low power) degrades plasmid DNA via strand scissions and crosslinking to yield nicked, linear, crosslinked and multiply fragmented plasmid DNA. Our experiments demonstrate the DNA degradation is power dependent and that at 100 W, a 1 min exposure will degrade less than 50 % of 1 μ g plasmid DNA. In contrast, a 200 W (1 min) exposure completely degrades the DNA until no longer detectable. This is significant since *D. radiodurans* can withstand ~ 150 strand breaks with no loss in viability (35). Hence, a 100 W exposure (which yielded a ~ 99.9 % sterilization of *D. radiodurans*) may not yield the necessary damage to the chromosome of the microbe; indicating that damage to other cellular components must also be a factor in sterilization. Model *in vitro* experiments demonstrate that plasma exposures also result in the rapid destruction of protein structure and abatement of enzymatic activity. Together, this supports a sterilization mechanism that proceeds through the degradation of both the surface and interior of *D. radiodurans*.

The sterilization, degradation and removal mechanisms occur as a result of several synergistic plasma processes. Comparison of the O₂ and Martian (CO₂) plasma experiments reveals that the role of chemical degradation is much greater than that of ion bombardment and UV photodesorption. Analysis on the plasma compositions indicates that atomic oxygen is in higher relative abundance in the O₂ plasma as expected, while the UV-B emissions are higher in the MAG plasma. The considerable difference in degree of microbial degradation (O₂ >> MAG) supports the role of atomic oxygen as the dominant source of degradation. However, the ~ 10-fold greater amount of DNA crosslinking induced by the Martian plasma, but comparable rates of DNA removal

($\text{MAG} \leq \text{O}_2$), supports the role of UV as the main source of DNA degradation at low plasma power. Which indicates that the ion bombardment and UV photodesorption processes are insufficient in causing significant damage to *D. radiodurans*. Thus, the sterilization and degradation of *D. radiodurans* must proceed through the primary action of chemically reactive species such as atomic oxygen and oxygen cation. Detection of carbonyl, sulfonate and alcohol reaction products support the oxidative degradation of *D. radiodurans* by reactive oxygen species.

Cold plasmas possess several advantages over most currently used techniques due to the volatilization chemistries that result from the degradation. Emission spectroscopy experiments show that *D. radiodurans* degrades into several low molecular weight species when exposed to the O_2 plasma. Conversion of the microbe into CO_2 , CO, N_2 , OH and H occurs as a synergistic effect of chemical degradation, ion bombardment and UV photodesorption. Detection of Na and K emission lines indicates that the redox chemistries of free electrons within the plasma further contribute to the degradation process. The detection of carbon and nitrogen species confirms the volatilization of biological matter and supports the observed loss of sample in the AFM, IR and biochemical experiments. Therefore, overexposures with the O_2 plasma result in both the sterilization and cleaning of contaminated surfaces.

Thus, we recommend oxygen plasmas for Planetary Protection procedures due to their demonstrated sterilization and cleaning efficacies. The rates of these processes are dependent on applied power, which can be adjusted to match material compatibility. Experiments using CO_2 plasma suggest that *D. radiodurans* may not be significantly degraded in an ionizing Martian atmosphere, which emphasizes the need for Planetary

Protection. Our DNA and protein experiments further indicate that O₂ plasmas have application in the sterilization and removal of viruses and protein toxins, such as HIV (36) and prions (11), respectively. Therefore, cold plasmas are important new tools for both astrobiology and medicine.

Acknowledgements

We thank Jeff Iland for construction of the ARC-PR, Brett Cruden for valuable discussions, and JPL () and the NASA Faculty Fellowship Program for support.

Abbreviations: ARC, Ames Research Center; UV, ultraviolet; SAB/BME, sample application buffer with β -mercaptoethanol

[†] A. A. Bol'shakov is a National Research Council Associate and on leave from Institute of Physics, St. Petersburg State University, St. Petersburg, 198904 Russia.

****** To whom reprints requests should be addressed at: MS: 239-15, Moffett Field, CA 94035. Email: jtrent@mail.arc.nasa.gov

References

1. Alfa, M. J. (2000) *Gastrointest. Endosc. Clin. N. Am.* **10**, 361-378.
2. Dempsey, D. J. & Thirucote, R. R. (1989) *J. Biomater. Appl.* **3**, 454-523.
3. DeVincenzi, D. L., Stabekis, P. & Barengoltz, J. (1996) *Adv. Space Res.* **18**, 311-316.
4. Rummel, J. D. (1992) *Adv. Space Res.* **12**, 129-131.
5. Mann, A., Kiefer, M. & Leuenberger, H. (2001) *J. Pharm. Sci.* **90**, 275-287.
6. Rutala, W. A. & Weber, D. J. (1999) *Infect. Control Hosp. Epidemiol.* **20**, 69-76.
7. Jacobs, G. P. (1995) *J. Biomater. Appl.* **10**, 59-96.
8. Akterian, S. G., Fernandez, P. S., Hendrickx, M. E., Tobback, P. P., Periago, P. M. & Martinez, A. (1999) *Int. J. Food. Microbiol.* **47**, 51-57.
9. Hoff, J. C. & Akin, E. W. (1986) *Environ. Health Perspect.* **69**, 7-13.
10. Buchanan, R. L., Edelson, S. G. & Boyd, G. (1999) *J. Food. Prot.* **62**, 219-228.
11. Antloga, K., Meszaros, J., Malchesky, P. S. & McDonnell, G. E. (2000) *ASAIO J.* **46**, S69-72.
12. Rutala, W. A. & Weber, D. J. (2001) *Emerg. Infect. Dis.* **7**, 348-353.
13. Doue, B. (1992) *Med. Device Technol.* **3**, 48-53.
14. Wallen, R. D., May, R., Rieger, K., Holloway, J. M. & Cover, W. H. (2001) *Biomed. Instrum. Technol.* **35**, 323-330.
15. Dillow, A. K., Dehghani, F., Hrkach, J. S., Foster, N. R. & Langer, R. (1999) *Proc. Natl. Acad. Sci. U S A* **96**, 10344-10348.
16. Zafar, A. B. (1996) *Am. J. Infect. Control* **24**, 312.
17. Adler, S., Scherrer, M. & Daschner, F. D. (1998) *J. Hosp. Infect.* **40**, 125-134.

18. Lerouge, S., Wertheimer, M. R., Marchand, R., Tabrizian, M. & Yahia, L. (2000) *J. Biomed. Mater. Res.* **51**, 128-135.
19. Jacobs, P. & Kowatsch, R. (1993) *Endosc. Surg. Allied Technol.* **1**, 57-58.
20. Moisan, M., Barbeau, J., Moreau, S., Pelletier, J., Tabrizian, M. & Yahia, L. H. (2001) *Int. J. Pharm.* **226**, 1-21.
21. Rummel, J. D. (2001) *Proc. Natl. Acad. Sci. U S A* **98**, 2128-2131.
22. Demidov, V. V., Goncharov, A. A., Osipov, V. B. & Trofimov, V. I. (1995) *Adv. Space Res.* **15**, 251-255.
23. Horneck, G., Facius, R., Reitz, G., Rettberg, P., Baumstark-Khan, C. & Gerzer, R. (2001) *Acta Astronaut* **49**, 279-288.
24. Lange, C. C., Wackett, L. P., Minton, K. W. & Daly, M. J. (1998) *Nat Biotechnol* **16**, 929-933.
25. Venkateswaran, A., McFarlan, S. C., Ghosal, D., Minton, K. W., Vasilenko, A., Makarova, K., Wackett, L. P. & Daly, M. J. (2000) *Appl. Environ. Microbiol.* **66**, 2620-2626.
26. Melin, A. M., Perromat, A. & Deleris, G. (2001) *Arch. Biochem. Biophys.* **394**, 265-274.
27. Chapman, B. (1980) *Glow Discharge Processes*. (John Wiley & Sons, Inc., New York).
28. Davies, K. J. (1987) *J. Biol. Chem.* **262**, 9895-9901.
29. Peskin, A. V. (1997) *Biochemistry (Mosc)* **62**, 1341-1347.
30. Garrison, W. M. (1987) *Chem. Rev.* **87**, 381-398.
31. Caimi, P. & Eisenstark, A. (1986) *Mutat. Res.* **162**, 145-151.

32. Hieda, K., Suzuki, K., Hirono, T., Suzuki, M. & Furusawa, Y. (1994) *J. Radiat. Res. (Tokyo)* **35**, 104-111.
33. Stevens, R., Nguyen, C., Cassell, A., Delzeit, L., Meyyappan, M. & Han, J. (2000) *Appl. Phys. Lett.* **77**, 3453-3455.
34. Silverstein, R. M., Bassler, G. C. & Morrill, T. C. (1991) *Spectrometric identification of organic compounds*. (John Wiley & Sons, Inc., New York).
35. Daly, M. J., Ouyang, L., Fuchs, P. & Minton, K. W. (1994) *J. Bacteriol.* **176**, 3508-3517.
36. Smith, R. A., Ingels, J., Lochemes, J. J., Dutkowsky, J. P. & Pifer, L. L. (2001) *J. Orthop. Res.* **19**, 815-819.

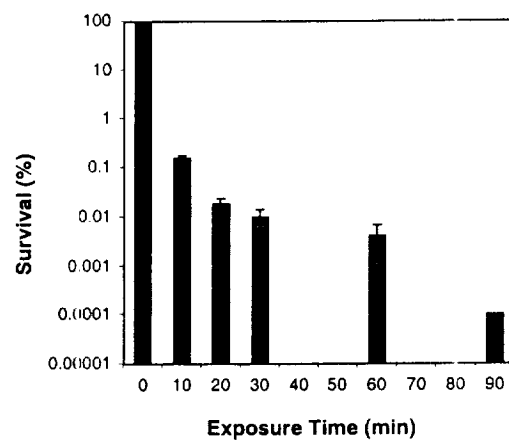


Fig. 1. Sterilization kinetics of *D. radiodurans* survival after exposure to O_2 plasma (≤ 25 W, ~ 45 mTorr).

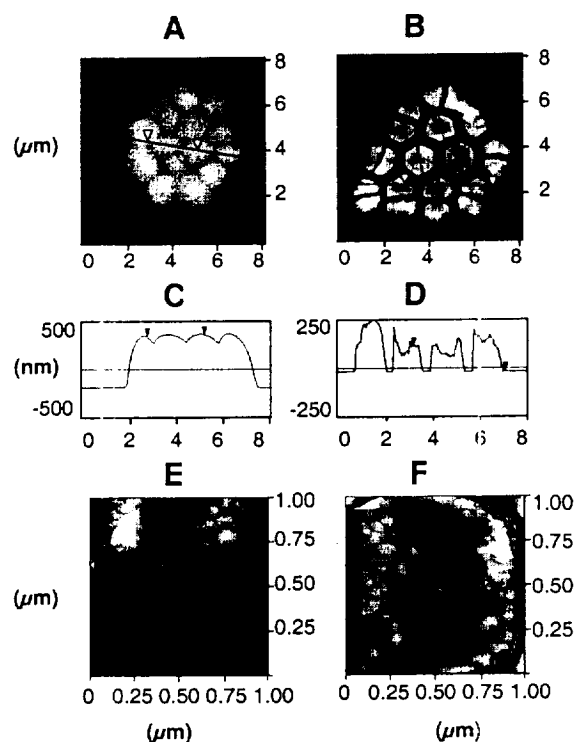


Fig. 2. AFM images of a *D. radiodurans* cell cluster (A) dried at 500 mTorr for 3 min and (B) after exposure to O₂ plasma (100 W, 500 mTorr, 3 min). Surface topography maps of each cluster were then obtained across the black line and between the inverted triangles of (C) the unexposed dried cell cluster and (D) the plasma exposed cell cluster. High-resolution images of (E) one dried cell and a (F) plasma exposed cell within each cluster were also obtained.

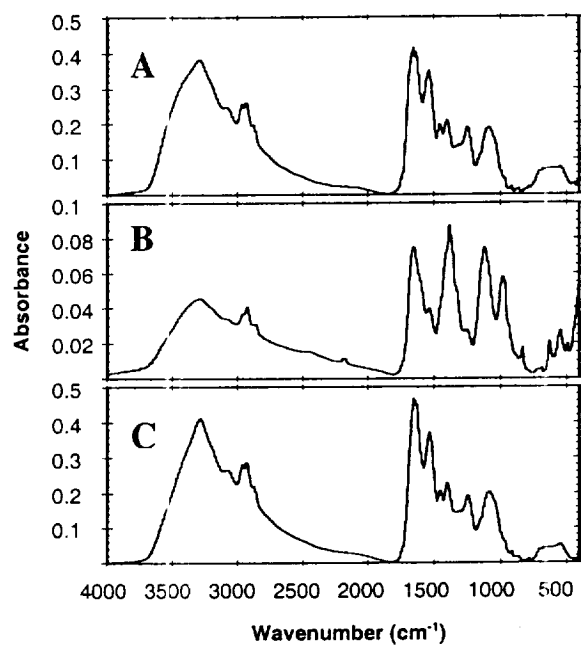


Fig. 3. Infrared spectra of *D. radiodurans*: (A) Control sample, (B) sample exposed to O₂ plasma and (C) sample exposed to MAG plasma. Plasma exposures were performed at 100 W and 500 mTorr for 45 min. Spectra have been displayed on differing scales for clarity.

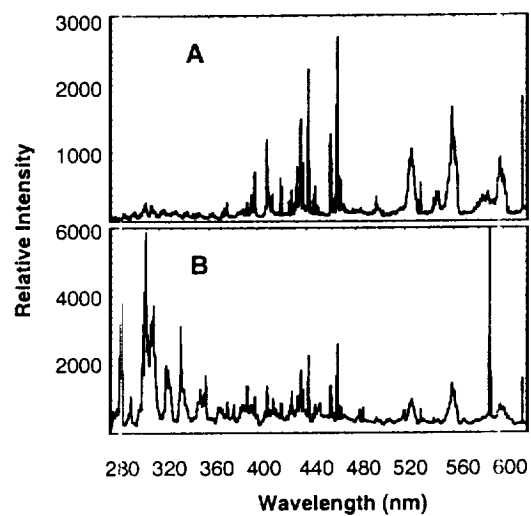


Fig. 4. Emission spectra of (A) pure O₂ plasma discharge and of (B) plasma during exposure of $\sim 10^9$ cells of *D. radiodurans* (100 W, 500 mTorr). Spectra are displayed from 280-620 nm and on differing scales for clarity.

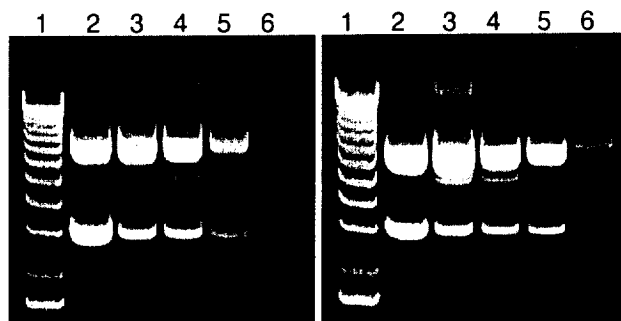


Fig. 5. Power dependent degradation of DNA by (A) O_2 and (B) MAG plasmas (60 s exposures). Lane 1, 1 kb DNA ladder; lane 2, DNA thermal control; lane 3, 50 W; lane 4, 100 W; lane 5, 150 W; lane 6, 200 W.

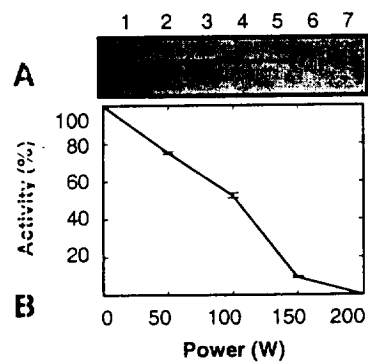


Fig. 6. Power dependent degradation of protein by O_2 plasma: (A) SDS-PAGE analysis of BSA degradation (0-250 W, 500 mTorr, 90 s). Lane 1, MW ladder; lane 2, BSA control; lane 3, 50 W; lane 4, 100 W; lane 5, 150 W; lane 6, 200 W; lane 7, 250 W. (B) Kinetic analysis of SLO degradation (0-200 W, 500 mTorr, 60 s).